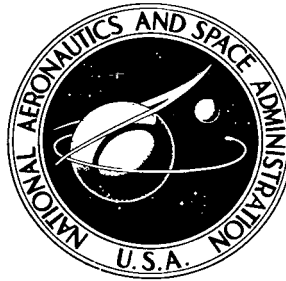


NASA TECHNICAL NOTE



NASA TN D-5998

c/

LOAN COPY: RET
AFWL (WLOI)
KIRTLAND AFB,



TECH LIBRARY KAFB, NM

NASA TN D-5998

OPTIMUM TRAJECTORIES TO CIRCULAR SYNCHRONOUS EQUATORIAL ORBIT FOR SMALLER-THAN-OPTIMUM APOGEE MOTORS

by Omer F. Spurlock and Fred Teren

*Lewis Research Center
Cleveland, Ohio 44135*



0132801

1. Report No. NASA TN D-5998	2. Government Accession No.	3. Recipient's Catalog No.	
4. Title and Subtitle OPTIMUM TRAJECTORIES TO CIRCULAR SYNCHRONOUS EQUATORIAL ORBIT FOR SMALLER-THAN-OPTIMUM APOGEE MOTORS		5. Report Date September 1970	6. Performing Organization Code
7. Author(s) Omer F. Spurlock and Fred Teren	8. Performing Organization Report No. E-5732		10. Work Unit No. 180-06
9. Performing Organization Name and Address Lewis Research Center National Aeronautics and Space Administration Cleveland, Ohio 44135		11. Contract or Grant No.	
12. Sponsoring Agency Name and Address National Aeronautics and Space Administration Washington, D. C. 20546		13. Type of Report and Period Covered Technical Note	
15. Supplementary Notes		14. Sponsoring Agency Code	
16. Abstract Analysis, procedure, and results are presented for maximizing payload capability for trajectories to circular synchronous equatorial orbit where the apogee motor total impulse is much smaller than optimum. The trajectories begin at launch and are numerically integrated to insertion into the final orbit. Constraints on parking orbit perigee radius and duration are included. These trajectories, unlike conventional synchronous orbit trajectories, were found to require noncircular parking orbits and large amounts of inclination reduction before the apogee burn. The analysis and procedure were also applied to the conventional circular synchronous equatorial orbit problem where the burn and coast durations are optimum. Results are presented for the Applications Technology Satellite (ATS)-E mission, which is an example of a problem where the apogee motor is small, and for the conventional case where the apogee motor is of optimum size.			
17. Key Words (Suggested by Author(s)) Optimum trajectories Calculus of variations Synchronous orbit Trajectory		18. Distribution Statement Unclassified - unlimited	
19. Security Classif. (of this report) Unclassified	20. Security Classif. (of this page) Unclassified	21. No. of Pages 28	22. Price* \$3.00

OPTIMUM TRAJECTORIES TO CIRCULAR SYNCHRONOUS EQUATORIAL ORBIT FOR SMALLER-THAN-OPTIMUM APOGEE MOTORS

by Omer F. Spurlock and Fred Teren

Lewis Research Center

SUMMARY

Analysis, procedure, and results are presented for maximizing the payload capability for trajectories to circular synchronous equatorial orbit where the apogee motor total impulse is much smaller than optimum. The trajectories begin at launch and are numerically integrated to insertion into the final orbit. Constraints on parking orbit perigee radius and duration are included as part of the solution. The trajectories, unlike conventional synchronous orbit trajectories, were found to require noncircular parking orbits and large amounts of inclination reduction before the apogee burn. A calculus of variations formulation of the optimization problem is used to obtain the solution.

Results are presented for the Applications Technology Satellite (ATS)-E mission, a circular synchronous equatorial orbit mission. The total impulse of the solid apogee motor is much smaller than optimum. The spacecraft mass for this mission was fixed. A conventional trajectory could not place the spacecraft in the required orbit. The unconventional trajectory was determined to be able to achieve the orbit.

The analysis and procedure were also applied to the conventional circular synchronous equatorial orbit problem where the burn and coast durations are optimum. Results are presented for a mission of this type to show that the familiar conventional circular synchronous equatorial orbit launch profile is essentially optimum.

INTRODUCTION

A conventional trajectory to circular synchronous equatorial orbit consists of five consecutive phases as shown in figure 1. The first phase is an ascent from the launch site to a circular parking orbit. To maximize the mass in parking orbit, a 90° launch azimuth is used, which results in a parking orbit inclination equal to the launch site latitude. This inclination must be removed during the trajectory. The second phase

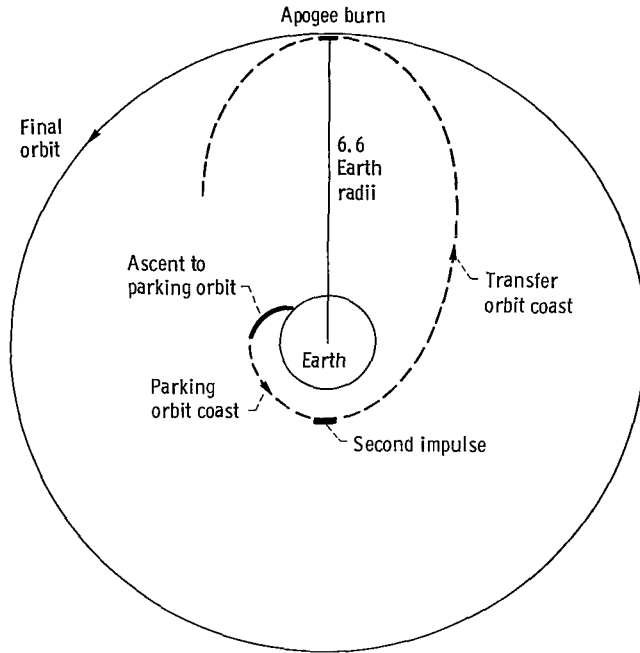


Figure 1. - Conventional trajectory to circular synchronous equatorial orbit. (Plane changes are not shown.)

is a coast arc to the proximity of the equator. A small portion of the required plane change is removed by the second burn, the third phase. Much more importantly, the second burn must place the vehicle in a transfer orbit whose apogee is over the equator and equal to synchronous altitude. The vehicle coasts to apogee of the transfer orbit in the fourth phase. The fifth phase consists of a final burn that removes the major portion of the inclination and circularizes the orbit. Intuitively, it seems reasonable that this conventional profile is near optimum if the burn and coast durations may be varied to maximize the mass at the end of each burn. However, if the total impulse of the final burn is fixed at less than the optimum value, the conventional trajectory must be modified to yield maximum payload to the final orbit. In particular, the parking orbit is noncircular, the perigee radius of the transfer orbit increases, and the second burn removes more than a minor part of the inclination. The optimization problem is to find the best combination of these changes and other less important ones to yield maximum payload to circular synchronous equatorial orbit.

Optimization of the conventional trajectory to circular synchronous equatorial orbit has been treated by several authors. Hoelker and Silber (ref. 1) present a detailed analysis of the conventional problem. Rider (ref. 2) considers the problem of changing the plane and also the radius of a circular orbit. These and other similar studies treat the problem as one of changing the plane and radius of a circular orbit, ignoring the

ascent to the first (parking) circular orbit. This is satisfactory for the conventional case. However, an unconventional trajectory is more complex since the parking orbit is in general noncircular. The ascent must be included as part of the optimization problem. Therefore, a more sophisticated optimization procedure is required for unconventional trajectories. Additionally, references 1 and 2 are general and consequently are not concerned with constraints which may alter the acceptability of a given trajectory, such as limitations on coast time or the minimum perigee radius of the noncircular parking orbit.

The problem of optimizing trajectories to circular synchronous equatorial orbit may be considered as a multistage launch vehicle optimization in which two or more of the burns and coasts are free for optimization. Several analyses have been performed to optimize multistage launch vehicles, including one by the authors of this report (ref. 3). For optimizing the unconventional trajectory, the analysis in reference 3 was expanded to three dimensions and, also, to include a perigee radius constraint on the parking orbit. The perigee radius constraint must be included to limit aerodynamic heating on the vehicle.

An example of a mission which requires an unconventional trajectory is the Applications Technology Satellite (ATS)-E mission on the Atlas-Centaur vehicle. The final burn is performed by a solid motor which is part of the spacecraft system. That motor is significantly smaller than optimum. There are spacecraft and launch vehicle constraints which must be incorporated into the solution. The perigee radius and the parking orbit coast duration are limited. The results for this problem are presented as an example of trajectory optimization for unconventional profiles.

The more complex analysis was also applied to a case where the apogee motor is of optimum size. References 1 and 2 show that the conventional trajectory is optimum if the ascent to parking orbit is ignored and if all burns are treated impulsively. This report examines the case where these simplifications are not made. An optimum trajectory is obtained and described.

ANALYSIS

Problem Description

A conventional trajectory to circular synchronous equatorial orbit consists of five phases:

- (1) Ascent to parking orbit
- (2) Parking orbit coast
- (3) Second impulse

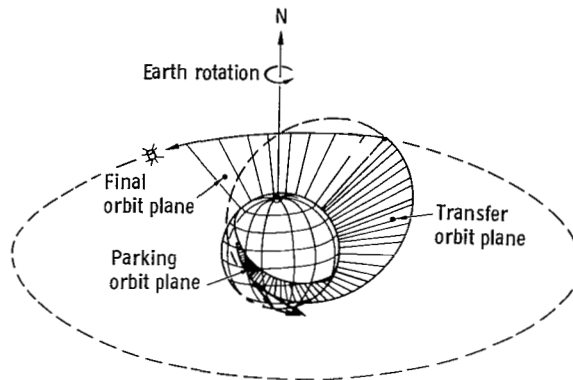


Figure 2. - Circular synchronous equatorial orbit ascent profile.

- (4) Transfer orbit coast
- (5) Third impulse or apogee burn

Figure 1 shows the planar characteristics of the conventional trajectory. The nonplanar characteristics are shown in figure 2.

The vehicle is launched at an azimuth of 90° in order to maximize the vehicle mass in parking orbit and to minimize the inclination of the parking orbit. The circular parking orbit altitude is as low as aerodynamic heating constraints will allow, usually about 165 to 185 kilometers. The parking orbit coast time is usually 15 minutes - the time required to coast from orbit insertion to the first equator crossing. The third phase places the vehicle in a transfer orbit whose apogee and perigee are over the equator. The apogee altitude is about equal to the required altitude for a circular synchronous orbit. The transfer orbit coast time is about $5\frac{1}{2}$ hours. The third impulse, the apogee burn, occurs at apogee of the transfer orbit. Apogee is designed to occur at the equator and at the proper altitude for injection into the final orbit. A small part of the inclination is removed by the second impulse with the remainder being removed by the apogee burn. In this conventional method, the final conditions at the end of each burn are known and the mass can easily be maximized progressively phase by phase if the second and third impulse sizes are unspecified.

Now suppose that the total impulse of the third burn is fixed. Then the transfer orbit must be constructed such that the ΔV available from the third impulse is exactly that required to place the vehicle in circular synchronous equatorial orbit. If the ΔV available from a fixed third total impulse is less than that required to circularize and equatorialize the orbit for the mass available from a conventional ascent and second impulse, then the trajectory to transfer orbit insertion must be altered to reduce the ΔV required of the third impulse. This can be done by reducing the required plane change and the ΔV required for circularization. For reasons described at length in the RESULTS AND DISCUSSION section, the unconventional trajectory needed to reduce the ΔV

required of the apogee motor varies in many respects from the conventional profile. The most dramatic changes are a noncircular parking orbit, nontrivial inclination reduction by the second impulse, and a significantly nonequatorial latitude for the second impulse. As is desired, the changes result in lowering the ΔV required of the fixed apogee motor. However, in this unconventional profile, the final conditions required at the end of the ascent and second impulse are unknown. They might be determined by varying those final conditions parametrically until the optimum is obtained. However, because of the number of variables, this process is clumsy and time consuming.

Calculus of Variations Solution

A calculus of variations formulation was used to maximize the payload to circular synchronous equatorial orbit without resorting to a parametric search. The optimization of the atmospheric portion of the trajectory is omitted from the variational analysis since the steering is severely constrained by aerodynamic loading and heating limitations. The analysis considers the problem from the point in the trajectory where the atmosphere can be neglected to insertion into the final orbit. In addition to optimizing the steering, the durations of any unspecified burns and coasts are optimized while maintaining the specified perigee radius of the parking orbit. The analysis is presented in appendix B. It is derived in three-dimensional rectangular coordinates in a manner similar to reference 4. The equations for optimum burn and coast duration are obtained from an analysis similar to that used in reference 3. It is necessary to extend the analysis to include an intermediate boundary condition which specifies the perigee radius of the parking orbit at the end of the ascent. Additionally, the oblate Earth model must be added to the variational analysis. The effect of oblateness is not negligible in trajectories to circular synchronous equatorial orbit. Trajectories to that orbit are long, minimally around 6 hours. Oblateness is the major perturbing force during most of a trajectory. Because of the large change in inclination required to perform the mission, any perturbation in the inclination, thus increasing or decreasing the amount of plane change required of the propulsion systems, affects the final mass and should be considered in the analysis.

The trajectories are numerically integrated to incorporate a nonimpulsive vehicle model and to include the effects of oblateness and small thrusts over long periods of time which cannot be conveniently treated impulsively.

The analysis presented in appendix B requires the solution of a two-point boundary value problem. The solution to the two-point boundary value problem for the circular synchronous orbit problem with a fixed apogee burn and parking orbit coast time requires satisfaction of a minimum of eight final conditions with an equal number of initial

conditions. The number and specific initial and final conditions are explained in appendix B.

Procedure

A simple Newton-Raphson iteration scheme was used to solve the two-point boundary value problem. This scheme was used successfully with as many as 12 iteration variables. For further explanation of the iteration scheme, see reference 5.

The partial derivatives required for the iteration scheme were obtained by integrating the adjoint equations. These were obtained as in reference 4. Solutions were initially obtained using a spherical Earth model for the adjoint equations, but it was found that including the oblateness terms improved the convergence properties of the problems. In some problems of this type, it was found that including the oblateness terms was necessary to obtain convergence.

It was difficult to obtain solutions to these problems because of the high degree of nonlinearity of many of the derivatives as well as the difficulty of guessing the initial values of the thrust angle in pitch and yaw and their rates. A technique was devised to systematically proceed from a simple, easily converged problem to the final solution. This technique is described at length in appendix C. Other techniques, such as gradient methods, might avoid some of the difficulties associated with the Newton-Raphson technique. However, the method described in the appendix is convenient, straightforward, and adequate. After getting one solution, proceeding to others in the region of interest is not difficult.

RESULTS AND DISCUSSION

The Applications Technology Satellite (ATS)-E mission is a circular synchronous equatorial orbit mission. The ATS program has the objective of advancing technology in areas which may have application to future spacecraft. The experiments which are conducted are spacecraft, technology, and science oriented.

The spacecraft-oriented experiments on the ATS-E provide information on power supply and control systems, a gravity-gradient stabilization system, resistojet and ion micropound thrusters, and synchronous environment. The technology-oriented experiments are primarily concerned with communication problems. The scientific-oriented experiments gather data on the particle (electron and proton) distribution and flux and the character of the electric and magnetic fields at synchronous altitude.

The launch vehicle for the ATS-E mission was an Atlas-Centaur and the solid apogee

motor was a part of the spacecraft system. The apogee motor total impulse was sized for the early ATS missions on the Atlas-Agena launch vehicle, which has less payload capability than the Atlas-Centaur. A desire to increase the spacecraft mass led to the change to the Atlas-Centaur. The apogee motor, although smaller than optimum for the larger vehicle, remained unchanged.

The Atlas-Centaur is a two-and-a-half stage vehicle. The Atlas is propelled by two booster engines and one sustainer engine. The booster engines are jettisoned at a pre-determined acceleration level. The sustainer engine continues to burn (sustainer solo). The Centaur insulation panels and then the payload fairing are jettisoned during this phase. The sustainer solo ends at propellant depletion and the Atlas stage is jettisoned. After about 10 seconds, the Centaur engines, burning hydrogen and oxygen, ignite and burn until the desired parking orbit is reached. During the parking orbit, a hydrogen peroxide propulsion system is used to maintain a very small acceleration for propellant retention and for attitude control. At the end of the parking orbit, the Centaur engines burn again until the proper transfer orbit is achieved. After engine shutdown, the Centaur control system acquires the proper orientation for the spacecraft burn, the Centaur and the spacecraft separate, and the spacecraft is spun up for stability. The spacecraft coasts up to the proper altitude maintaining the separation attitude. The spacecraft motor burns to place the spacecraft in the final orbit. The spacecraft apogee motor has a thrust of 22 240 newtons and an effective specific impulse of 279.1 seconds. The total impulse available from the motor is 950 900 newton-seconds, which corresponds to a propellant load of 347 kilograms.

The trajectory starts with a short vertical rise followed by a rapid pitchover phase in the desired azimuth direction. The amount of pitchover determines the amount of lofting during the atmospheric portion of the trajectory. The remainder of the atmospheric phase (which is assumed to end at booster stage jettison) is flown with a near-zero angle of attack steering program (described in ref. 5) to minimize vehicle heating and aerodynamic loads. The thrust direction is constrained to be parallel to the launch azimuth plane, which is established at launch.

Since the ATS-E spacecraft motor has a fixed propellant load, the trajectory must be designed such that the ΔV required at apogee of the transfer orbit is exactly that required to place the spacecraft in the desired final orbit. As mentioned earlier, the ATS-E motor is much smaller than optimum. The Atlas-Centaur can put more mass in a conventional transfer orbit than the apogee motor can place in circular synchronous equatorial orbit. Therefore, an unconventional trajectory is required to lower the ΔV required of the apogee burn.

An optimum unconventional trajectory was obtained for the ATS-E mission to circular synchronous equatorial orbit. The ΔV required of the apogee motor is reduced by decreasing each of the two components which together make up the total ΔV - that

needed to circularize the orbit and to reduce the inclination to zero. The ΔV for circularization is reduced by increasing the horizontal velocity at apogee of the transfer orbit without adding radial velocity. Any radial velocity would have to be removed by the apogee burn. Increasing the horizontal velocity at a fixed apogee radius is equivalent to raising the perigee radius of the transfer orbit - thereby decreasing the ellipticity of the transfer orbit.

The ΔV required at apogee for reducing the inclination to zero is decreased by lowering the inclination of the transfer orbit. However, raising the velocity at apogee increases the ΔV required for inclination removal at a fixed transfer orbit inclination. Therefore, the combination of the two methods represents a compromise which is optimized as part of the total problem. Most of the inclination reduction is performed by the second burn near the equator and only a small part is accomplished in the ascent to parking orbit.

The characteristics of the optimum parking orbit are changed from the conventional profile to increase the perigee radius of the transfer orbit. An elliptical rather than circular parking orbit is used to raise the altitude of the second burn. The perigee radius of the optimum parking orbit remains limited by aerodynamic heating considerations at some acceptable value. Since injection into the parking orbit occurs near perigee, the vehicle must coast along the ellipse to a higher radius. Because of the limitation of the coast duration for the ATS-E mission, the second burn was required to occur near the first equator crossing. (From tracking or other considerations, a second (or greater) equator crossing could be chosen for the second burn, which would increase the parking orbit coast time by a half period (or more).) The latitude of the second burn is no longer equatorial as in the conventional case since the optimum position for raising the perigee radius and decreasing the inclination is dependent on radius and velocity as well as latitude. The parking orbit coast time is greater for this unconventional profile since the time to the equator is greater for an elliptical than for a circular parking orbit and, additionally, the second burn occurs significantly south of the equator. Optimum true anomalies are found for the beginning and end of the parking and transfer orbit coasts. In addition, the optimum combination of the changes just described as characterizing the unconventional profile is selected.

The desired final inclination for the ATS-E mission is not exactly zero. The perturbations of the Sun, Moon, and oblateness of the Earth cause a spacecraft to drift from an exactly equatorial orbit. Since zero inclination is not a stable condition, a final orbit inclination yielding the smallest average inclination over the lifetime of the spacecraft is desired. Small final inclinations with the proper inertial ascending node are found to yield acceptable inclination over the lifetime of the satellite. The particular combinations of final orbit inclination and ascending node are functions of the positions of the Sun and Moon, which are in turn functions of launch time and date. Therefore, data

were obtained for payload to circular synchronous orbits as a function of final inclination. Negative inclinations are included in the data. This convention indicates that the node has been switched approximately 180° by the apogee burn.

The Atlas-Centaur has a 25-minute limitation on parking orbit coast time for the mission. Therefore, inclusion of that constraint is necessary for realistic determination of vehicle capability. However, optimizing the coast time provides a more dramatic and obvious demonstration of the optimization procedure.

Figure 3 presents separated spacecraft mass as a function of launch azimuth for

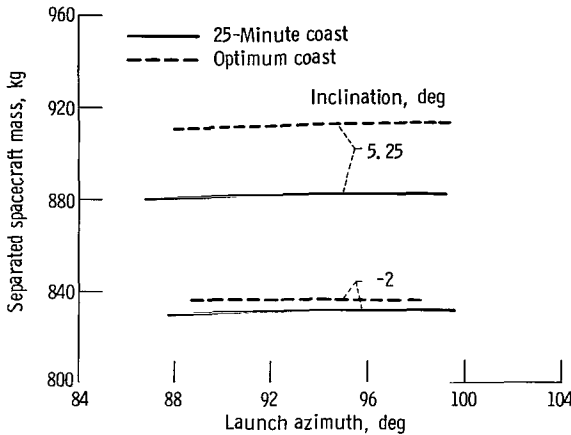


Figure 3. - Separated spacecraft mass as function of launch azimuth.

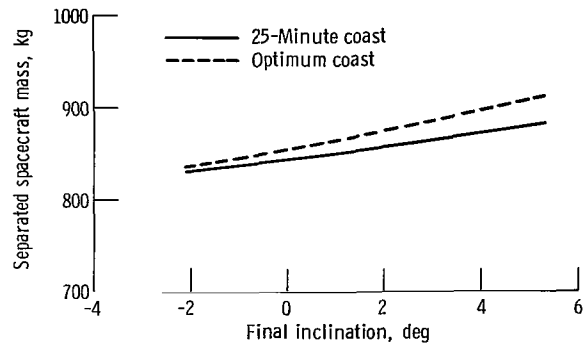


Figure 4. - Separated spacecraft mass as function of final inclination.

final inclinations of $(-)2^\circ$ and 5.25° for both optimum and 25-minute parking orbit coast times. Separated spacecraft mass is the mass of the spacecraft when it is separated from the Centaur vehicle. This figure shows that the separated spacecraft mass is rather insensitive to launch azimuth. Hence, for simplicity, launch azimuth is fixed at 90° for the remaining figures.

Figure 4 shows the separated spacecraft mass as a function of final inclination. The separated spacecraft mass decreases as final inclination decreases. Figures 5 and 6 show the effect of final inclination on the transfer orbit inclination and inertial velocity at apogee. As might be expected, as the final inclination decreases, so does the transfer orbit inclination because of the nearly fixed amount of inclination change supplied by the small apogee motor.

As might not be expected, the velocity at apogee also decreases as final inclination decreases, especially for the case of optimum coast times. Figures 7 to 12 show why this occurs. Figure 7 shows the latitude of the second Centaur engine start as a function of final inclination. Since the second burn is required to remove more inclination as final

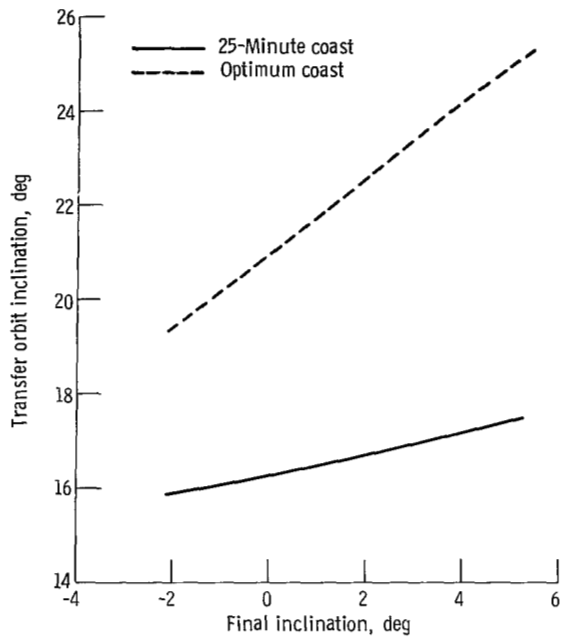


Figure 5. - Transfer orbit inclination as function of final inclination.

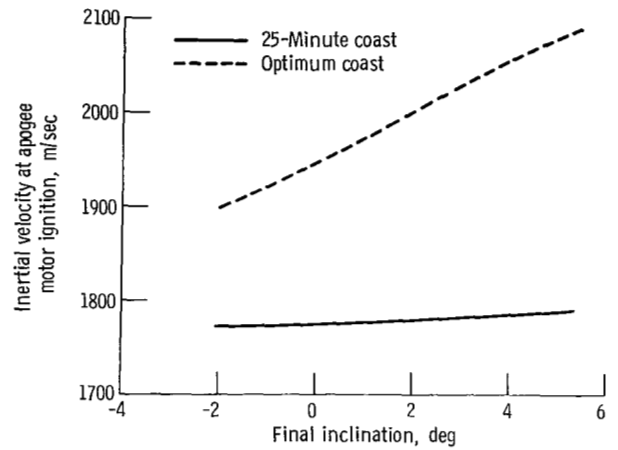


Figure 6. - Inertial velocity at apogee motor ignition as function of final inclination.

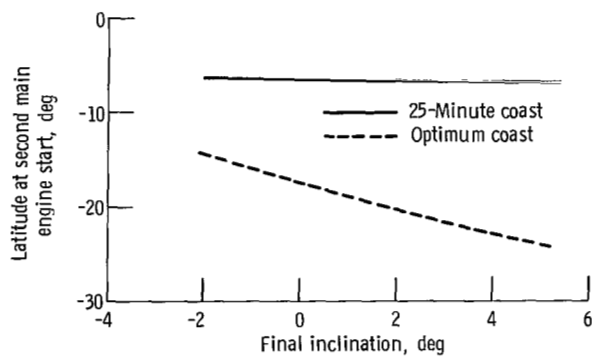


Figure 7. - Latitude at second main engine start as function of final inclination.

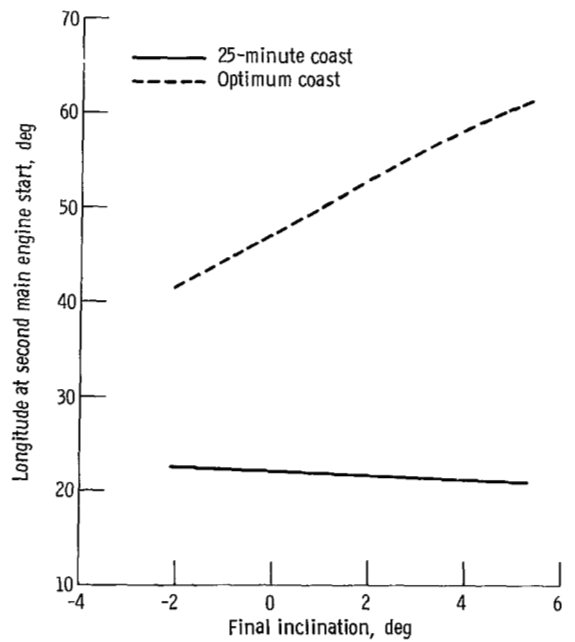


Figure 8. - Longitude at second main engine start as function of final inclination.

inclination decreases, it is advantageous to move the burn nearer the equator for more efficient plane change. Figure 8 shows that the longitude of second burn start also decreases as final inclination decreases. These trends decrease the parking orbit coast arc as final inclination decreases. This is reflected in a decrease in the true anomaly at second Centaur cutoff, as seen in figure 9. Figures 10 to 12 show additional effects

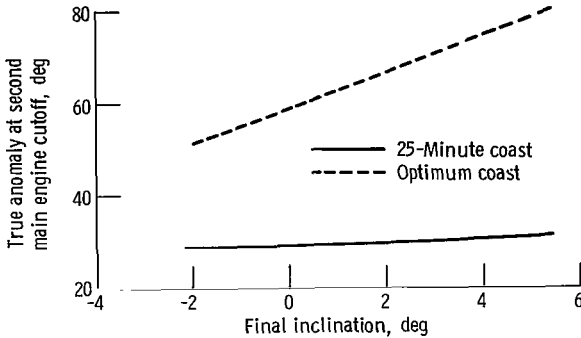


Figure 9. - True anomaly at second main engine cutoff as function of final inclination.

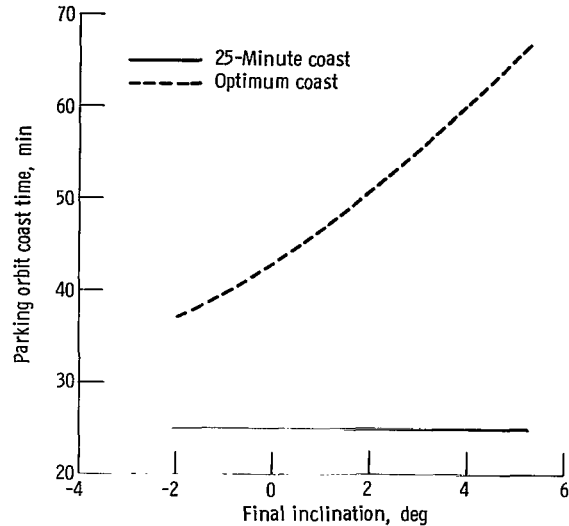


Figure 10. - Parking orbit coast time as function of final inclination.

of moving the second burn nearer the equator. It decreases the parking orbit coast time, the altitude of the second burn, and the apogee altitude of the parking orbit. These all occur as a result of the decrease in parking orbit coast arc. These figures show why the apogee velocity is decreasing as final inclination decreases. The perigee radius of the transfer orbit decreases as the altitude of the second burn decreases. The apogee altitude of the transfer orbit is almost constant at synchronous altitude; hence, as perigee decreases, so does apogee velocity.

Figures 5 and 6 also indicate that more ΔV is required of the apogee motor as final inclination decreases. It can be seen that both the plane change and circularization ΔV are increasing. However, figure 4 shows that the spacecraft ignition mass is decreasing, which increases the ΔV capability of the apogee motor.

Figure 13 shows the percentage of the Centaur propellant used in the first burn. The figure shows that as the final inclination increases, the first burn duration increases as the apogee altitude increases (fig. 12).

The final longitude as a function of final inclination is shown in figure 14. The satellite remains at the longitude indicated only when the inclination is zero, the orbit cir-

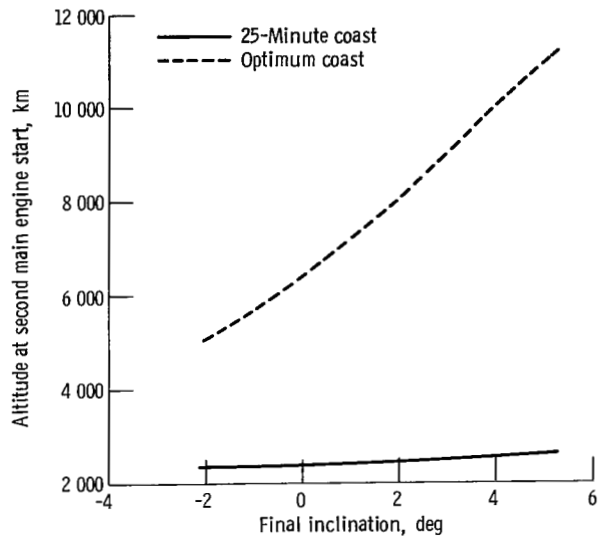


Figure 11. - Altitude at second main engine start as function of final inclination.

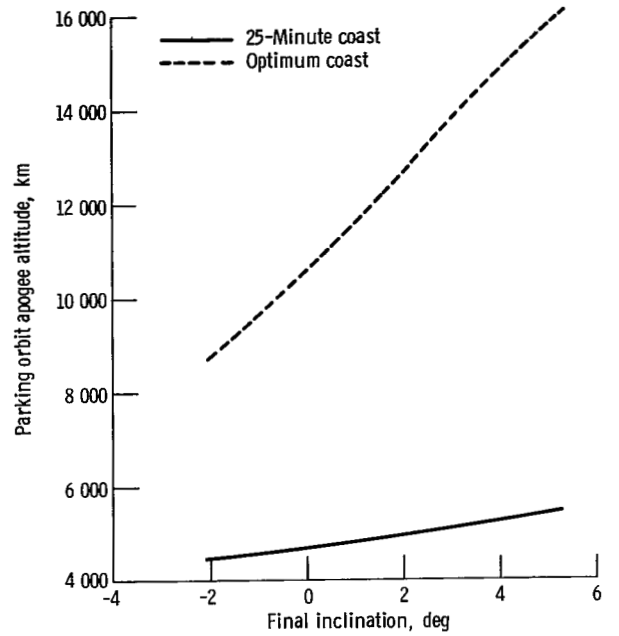


Figure 12. - Parking orbit apogee altitude as function of final inclination.

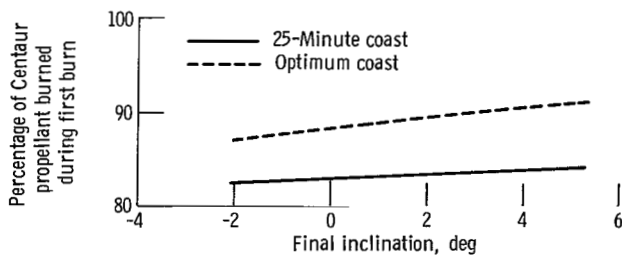


Figure 13. - Percentage of Centaur propellant burned during first burn as function of final inclination.

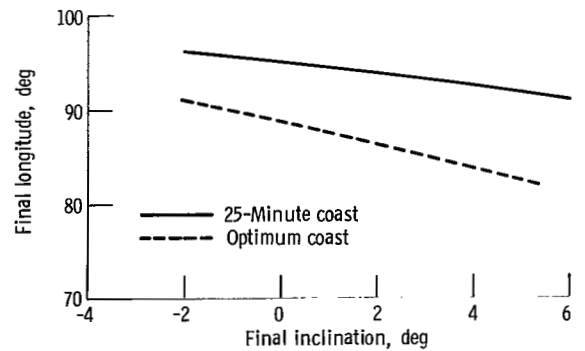


Figure 14. - Final longitude as function of final inclination.

cular, and the altitude synchronous. For other inclinations, the position (latitude and longitude) of the satellite subpoint describes a figure eight on the surface of the rotating Earth. The longitudes indicated in figure 14 are injection longitudes, not necessarily the longitude at which the equator crossing occurs. For small inclinations, the longitude does not vary greatly during the period of the orbit. Figure 14 shows that longitude decreases as final inclination increases.

Now consider the limitation of parking orbit coast time. Twenty-five minutes is less than optimum for all the final inclinations considered, as seen in figure 10. The difference in separated spacecraft mass is shown in figure 4. As seen from these figures, as the difference between the optimum and limited coast times decreases, the loss in payload due to coast time limitation decreases also.

The coast time limitation reduces the advantage of raising the apogee of the parking orbit as final inclination increases. The energy required to raise apogee does not yield the payload increases available with optimum coast time since altitude can not be acquired as efficiently in the shorter coast time. The energy is better spent by the second burn to reduce the inclination of the transfer orbit. This is reflected in several of the figures. In figure 5, the transfer orbit inclination for the coast limited case lies well below the optimum case. The lower second burn altitude is reflected in the lower velocity at apogee of the transfer orbit, as seen in figure 6. Because the parking orbit characteristics do not vary greatly with final inclination, the latitude and longitude of the second burn and the true anomaly at second Centaur cutoff are nearly constant. These may be seen in figures 7 to 9. The conclusions which may be drawn for the percentage of Centaur propellant used in the first burn and final longitude (figs. 13 and 14) are similar to those for the optimum coast case.

Conventional Circular Synchronous Equatorial Orbit Trajectories

The analysis and techniques developed to optimize the unconventional trajectory were applied to the conventional problem. References 1 and 2 show that the conventional trajectory profile for reaching a circular synchronous equatorial orbit is optimum if the second and third burns are impulsive and free for optimization. As mentioned in the INTRODUCTION, the referenced analyses assume that a circular orbit about a spherical Earth has already been achieved. The effects on the optimum profile of an oblate Earth, a nonimpulsive vehicle model, and the ascent to parking orbit were not considered. These effects are investigated with the present, more complex, analysis.

The vehicle model chosen for the second study is the Atlas-Centaur, except that the Centaur stage of the vehicle is simplified so that the trajectory characteristics will not be obscured by vehicle peculiarities. In particular, the Centaur stage is used with

constant thrust and specific impulse from Atlas sustainer jettison through injection into circular synchronous equatorial orbit. No solid apogee motor is used. All jettisoned weights were eliminated in that period and only the main engines were used. The parking and transfer orbit coasts were without thrust and mass flow.

The durations of the first, second, and third Centaur burns are optimized, as are the two coast phases. The resulting optimum trajectory had a circular parking orbit and the optimum launch azimuth was 91° . About 0.3° of inclination was removed during the ascent to the circular parking orbit. Although a 91° launch azimuth is only slightly better than using a 90° launch azimuth, moving the trajectory closer to the equator more quickly makes plane change in the ascent more advantageous. The second Centaur burn spans the equator and lowers the inclination by 2.1° . The remaining inclination is removed at apogee of the transfer orbit as the trajectory is circularized.

The analysis used for this conventional problem is identical to that used in the unconventional problem except for some modifications necessary because the optimum parking orbit is circular. The perigee altitude constraint becomes more complex for a circular orbit. This is treated in appendix B.

The results confirm that the conventional trajectory profile is essentially optimum even with an oblate Earth model and a nonimpulsive vehicle simulation.

SUMMARY OF CONCLUSIONS

Analysis and results are presented for trajectories to circular synchronous equatorial orbit where the apogee motor is fixed at a smaller than optimum total impulse and for a conventional optimum configuration. The results for the small apogee motor case were obtained for the ATS-E mission, which used the Atlas-Centaur launch vehicle.

The results confirm that the conventional trajectory profile is essentially optimum vehicle-apogee motor combinations where the apogee motor is smaller than optimum. More important, the results demonstrate that optimum trajectories to circular synchronous equatorial orbits may be obtained with detailed and hence complicated vehicle models for unconventional (small apogee motor) as well as conventional (optimum burn time) trajectory profiles. These results may be obtained without resorting to exotic mathematical procedures for solving the two-point boundary value problem. These results were obtained with a simple Newton-Raphson iteration scheme. The partial derivatives were obtained by integrating the adjoint equations. The simple iteration scheme with the integrated partial derivatives is able to obtain solutions to the highly nonlinear two-point boundary value problem even when the number of initial and final conditions reaches twelve.

The conventional circular synchronous equatorial orbit problem is also investigated

with the complex analysis used for the unconventional problem. The results demonstrate that the conventional trajectory is essentially optimum even with an oblate Earth model and a nonimpulsive vehicle simulation.

Lewis Research Center,
National Aeronautics and Space Administration,
Cleveland, Ohio, June 30, 1970,
180-06.

APPENDIX A

SYMBOLS

<p>C first integral of Euler-Lagrange equations, kg/sec</p> <p>E energy per unit mass, m^2/sec^2</p> <p>e eccentricity, dimensionless</p> <p>F functional defined by eq. (B4), kg/sec</p> <p>f unit thrust direction</p> <p>\bar{G} gravity acceleration, m/sec^2</p> <p>G_m^* spherical Earth gravity constant, m^3/sec^2</p> <p>\bar{G}_1, \bar{G}_2 components of oblate gravity acceleration, m/sec^2</p> <p>g intermediate boundary equation</p> <p>h angular momentum per unit mass, m^2/sec</p> <p>J functional to be minimized, kg</p> <p>m mass, kg</p> <p>N total number of stages</p> <p>p semilatus rectum, m</p> <p>r radius, m</p> <p>r_p perigee radius, m</p> <p>S variational switching function, dimensionless</p> <p>T thrust, N</p> <p>t time, sec</p> <p>v velocity, m/sec</p>	<p>\hat{z} unit vector pointing at north pole</p> <p>β mass flow rate, kg/sec</p> <p>ϵ jump factor</p> <p>η Lagrange multiplier, kg/sec</p> <p>λ Lagrange multiplier, kg-sec/m</p> <p>μ Lagrange multiplier, kg/m</p> <p>σ Lagrange multiplier, dimensionless</p> <p>φ yaw attitude, deg</p> <p>ψ pitch attitude, deg</p> <p>Superscripts:</p> <p>f final</p> <p>o initial</p> <p>. time derivative</p> <p>— vector</p> <p>^ unit vector</p> <p>Subscripts:</p> <p>d desired</p> <p>f final</p> <p>$\left. \begin{matrix} i, j, k, \\ l, m, n \end{matrix} \right\}$ stage numbers</p> <p>o initial</p> <p>pk parking orbit</p>
--	--

APPENDIX B

DERIVATION OF OPTIMUM CONTROL

As mentioned in the ANALYSIS section, the optimization of a trajectory to a circular synchronous equatorial orbit may be considered as the problem of optimizing a multistage launch vehicle to a particular final orbit. The optimization problem to be considered here begins at booster jettison, which is assumed to be at a fixed position and velocity. The sustainer portion of the Atlas continues until propellant depletion. The sustainer is jettisoned and a few seconds later the first Centaur burn begins. Its duration is variable and must be optimized. The perigee radius of the parking orbit which follows is fixed. The duration of the parking orbit may or may not be optimized. The parking orbit is not a true coast since a small acceleration is maintained for propellant retention. The duration of the second Centaur burn must be optimized, followed by an optimum transfer orbit coast (a true coast) and a final burn of fixed total impulse. The analysis presented in this appendix to solve this problem is a special case of the analysis in reference 3, with the additional constraint of a parking orbit perigee radius.

The variational problem to be solved is to find the steering program and various stage durations which maximize the payload capability of a multistage launch vehicle to a specified final orbit. The trajectory must satisfy certain initial, final, and intermediate conditions on the state variables. The thrust, propellant flow rate, and jettison weight for each stage are assumed to be constant. The equations of motion and constraints for each stage may be written as

$$\dot{\mathbf{v}} - \overline{\mathbf{G}}(\overline{\mathbf{r}}) - \frac{T_1}{m} \hat{\mathbf{f}} = \overline{\mathbf{0}} \quad (\text{B1a})$$

$$\dot{\overline{\mathbf{r}}} - \overline{\mathbf{v}} = \overline{\mathbf{0}} \quad (\text{B1b})$$

$$\dot{m} + \beta_1 = 0 \quad (\text{B1c})$$

$$\hat{\mathbf{f}} \cdot \hat{\mathbf{f}} - 1 = 0 \quad (\text{B1d})$$

where $\hat{\mathbf{f}}$ is the unit thrust direction and $\overline{\mathbf{G}}(\overline{\mathbf{r}})$ is the oblate Earth gravity acceleration (ref. 6), which may also be written

$$\overline{\mathbf{G}}(\overline{\mathbf{r}}) = G_1(r, \overline{\mathbf{r}} \cdot \hat{\mathbf{z}})\hat{\mathbf{r}} + G_2(r, \overline{\mathbf{r}} \cdot \hat{\mathbf{z}})\hat{\mathbf{z}} \quad (\text{B2})$$

Suppose that each stage of the vehicle is numbered consecutively starting with the booster. For analysis purposes a stage change occurs when the thrust and/or propellant flow rate changes and/or a mass is jettisoned. A Bolza formulation of the variational problem is used (ref. 7), and the functional to be minimized is written as in reference 3 as

$$J = -m_f + \sum_{i=2}^N \int_{t_{i-1}}^{t_i} F_i dt \quad (B3)$$

where the functional F_i for each stage is

$$F_i = \bar{\lambda} \cdot \left(\dot{\bar{v}} - \bar{G} - \frac{T_i}{m} \hat{f} \right) + \bar{\mu} \cdot (\dot{\bar{r}} - \bar{v}) + \sigma(\dot{m} + \beta_i) + \eta(\hat{f} \cdot \hat{f} - 1)$$

The resulting Euler-Lagrange equations are

$$\dot{\bar{\lambda}} + \bar{\mu} = \bar{0} \quad (B5a)$$

$$\dot{\bar{\mu}} + \frac{G_1 \bar{\lambda}}{r} + (\bar{\lambda} \cdot \hat{r}) \bar{\nabla}_{\bar{r}} G_1 - G_1 (\bar{\lambda} \cdot \hat{r}) \frac{\hat{r}}{r} + (\bar{\lambda} \cdot \hat{z}) \bar{\nabla}_{\bar{r}} G_2 = \bar{0} \quad (B5b)$$

$$\dot{\sigma} - \frac{T_i}{m^2} \bar{\lambda} \cdot \hat{f} = 0 \quad (B5c)$$

$$2\eta \hat{f} - \frac{T_i}{m} \bar{\lambda} = \bar{0} \quad (B5d)$$

The optimum thrust direction \hat{f} is obtained by combining equations (B5d) and (B5c) and using the Weierstrass E-test. This procedure results in

$$\hat{f} = \hat{\lambda} \quad (B6)$$

Integrals of the Motion

Since F does not explicitly depend on time, an integral of the motion is

$$C_i + \bar{\lambda} \cdot \bar{G} + \bar{\mu} \cdot \bar{v} + \frac{T_i}{m} \lambda - \sigma \beta_i = 0 \quad (\text{B7})$$

When a spherical gravity model is assumed (i. e. , $\bar{G}(\bar{r}) = (G_m^*/r^3)\bar{r}$), three additional integrals of the motion exist which are given by

$$\bar{\lambda} \times \bar{v} + \bar{\mu} \times \bar{r} = \overline{\text{constant}}$$

Since $\bar{\lambda}$, $\bar{\mu}$, \bar{r} , and \bar{v} are all continuous except where an intermediate boundary condition is imposed (as will be shown later), the three integrals are constant across staging points where continuity holds. However, for the oblate gravity model used in this analysis, only a single component of the previous vector integral is constant, as can be verified by differentiation with respect to time:

$$(\bar{\lambda} \times \bar{v} + \bar{\mu} \times \bar{r}) \cdot \hat{z} = \text{constant} \quad (\text{B8})$$

Transversality Equation

The transversality equation for this problem is

$$dJ = \sum_{i=2}^N (C dt + \bar{\lambda} \cdot d\bar{v} + \bar{\mu} \cdot d\bar{r} + \sigma dm)_{t_{i-1}}^{t_i} - dm_f \quad (\text{B9})$$

which is set equal to zero for an optimal solution. Reference 3 shows that $\bar{\lambda}$ and $\bar{\mu}$ are continuous everywhere if there are no intermediate boundary conditions. If the intermediate boundary condition (assumed to occur at a staging point) is expressed as

$$g(\bar{r}, \bar{v}) = 0 \quad (\text{B10})$$

reference 8 shows that the discontinuities in $\bar{\lambda}$ and $\bar{\mu}$ are $\epsilon \bar{\nabla}_{\bar{v}} g$ and $\epsilon \bar{\nabla}_{\bar{r}} g$, respectively. The variable ϵ is used as an initial condition in the two-point boundary value problem to satisfy the intermediate boundary condition (eq. (B10)).

The equations that must be satisfied to optimize the duration of the powered and coast stages are derived in reference 3. The applicable results are presented here. Let j be the first optimized powered stage. Then for constant jettison weight the equation for optimizing stage l is

$$\sum_{i=j}^{l-1} (S_i^f - S_{i+1}^o) = 0 \quad (\text{B11})$$

where o and f refer to initial and final values and the S functions are defined as

$$S_i \equiv \frac{C}{\beta_i} - \sigma = \frac{-\left(\bar{\lambda} \cdot \bar{G} + \bar{\mu} \cdot \bar{v} + \frac{T_i}{m} \lambda\right)}{\beta_i} \quad \text{for } \beta_i \neq 0 \quad (\text{B12a})$$

$$S_i \equiv 0 \quad \text{for } \beta_i = 0 \quad (\text{B12b})$$

The right side of equation (B12a) is obtained by using equation (B7). For coasting stages ($\beta_i = T_i = 0$) to be optimized, the equation

$$C_i = -(\bar{\lambda} \cdot \bar{G} + \bar{\mu} \cdot \bar{v}) = 0 \quad (\text{B13})$$

must be satisfied for maximum payload.

For free initial or final state variable x, the required or final condition for maximum payload (ref. 4) is

$$\bar{\lambda} \cdot \frac{\partial \bar{v}}{\partial x} + \bar{\mu} \cdot \frac{\partial \bar{r}}{\partial x} = 0 \quad (\text{B14})$$

Initial Conditions

If the initial position and velocity are specified, the initial values of any five of the six $\bar{\lambda}$ and $\bar{\mu}$ may be used as variable initial conditions to satisfy the required final conditions of the two-point boundary value problem. To eliminate the difficulty associated with guessing at values of the multipliers, the values of $\bar{\lambda}$ and $\bar{\mu}$ can be expressed in terms of pitch and yaw attitude (ψ and φ) and rates ($\dot{\psi}$ and $\dot{\varphi}$). These equations may be found in appendix C of reference 4. The values of $\bar{\lambda}$ and $\bar{\mu}$ are then calculated from

$$\bar{\lambda} = \lambda \hat{\lambda} \quad (\text{B15a})$$

$$\bar{\mu} = -\lambda \dot{\hat{\lambda}} - \dot{\lambda} \hat{\lambda} \quad (\text{B15b})$$

The value of λ can be set equal to unity without loss of generality. The initial value of $\dot{\lambda}$ can be calculated in closed form, as will be shown by the following development.

Final Conditions

Final conditions for both the conventional and unconventional synchronous equatorial orbit mission require a circular orbit at synchronous orbit altitude with prescribed inclination. If the required inclination is nonzero, both the longitude of the ascending node and the injection point in the final orbit are free for optimization. As shown in reference 4, the corresponding auxiliary variational final conditions are

$$(\bar{\lambda} \times \bar{v} + \bar{\mu} \times \bar{r}) \cdot \hat{z} = 0 \quad (\text{B16a})$$

and

$$(\bar{\lambda} \times \bar{v} + \bar{\mu} \times \bar{r}) \cdot (\bar{r} \times \bar{v}) = 0 \quad (\text{B16b})$$

If the desired inclination is zero, equations (B16a) and (B16b) degenerate into one equation (zero inclination is equivalent to two final conditions, $\bar{r} \cdot \hat{z} = 0$ and $\bar{v} \cdot \hat{z} = 0$), and only equation (B16a) must be satisfied.

Since equation (B16a) is a constant of the motion (eq. (B8)), it may be satisfied at the beginning of the trajectory and used to calculate $\dot{\lambda}$. However, it must first be verified that jump discontinuities in $\bar{\lambda}$ and $\bar{\mu}$ at intermediate boundary points do not change the value of the constant. This requires that

$$(\bar{v}_{\bar{v}g} \times \bar{v} + \bar{v}_{\bar{r}g} \times \bar{r}) \cdot \hat{z} = 0 \quad (\text{B17})$$

It will be shown later that equation (B17) is satisfied for all functions g used herein.

The calculation of $\dot{\lambda}$ proceeds as follows:

$$\begin{aligned} (\bar{\lambda} \times \bar{v} + \bar{\mu} \times \bar{r}) \cdot \hat{z} &= (\lambda \hat{\lambda} \times \bar{v}) \cdot \hat{z} - (\lambda \hat{\lambda} \times \bar{r}) \cdot \hat{z} - (\dot{\lambda} \hat{\lambda} \times \bar{r}) \cdot \hat{z} = 0 \\ \dot{\lambda} &= \frac{\lambda(\hat{\lambda} \times \bar{v} - \hat{\lambda} \times \bar{r}) \cdot \hat{z}}{(\hat{\lambda} \times \bar{r}) \cdot \hat{z}} \end{aligned} \quad (\text{B18})$$

Computing $\dot{\lambda}$ with equation (B18) guarantees that equation (B16a) will be satisfied.

Intermediate Conditions

As explained earlier, it is necessary to constrain the perigee radius at injection into the first parking orbit. Otherwise, the optimum solution would result in the parking orbit injection and/or the equator crossing occurring at very low altitudes, thus violating spacecraft heating constraints. Therefore, the intermediate constraint is

$$g(\bar{r}, \bar{v}) = r_p - r_{p,d} = 0 \quad (\text{B19})$$

where the desired value corresponds to the perigee altitude. If equations found in reference 9 are used, equation (B19) can be written as

$$\frac{p}{1+e} - r_{p,d} = 0 \quad (\text{B20})$$

where

$$p = \frac{\bar{h} \cdot \bar{h}}{G_m^*} \quad (\text{semilatus rectum}) \quad (\text{B21a})$$

$$e = \sqrt{1 + \frac{2E_p}{G_m^*}} \quad (\text{eccentricity}) \quad (\text{B21b})$$

$$E = \frac{\bar{v} \cdot \bar{v}}{2} - \frac{G_m^*}{r} \quad (\text{energy per unit mass}) \quad (\text{B21c})$$

$$\bar{h} = \bar{r} \times \bar{v} \quad (\text{angular momentum per unit mass}) \quad (\text{B21d})$$

The required gradients are calculated to be

$$\bar{\nabla}_{\bar{v}} g = \frac{h(\hat{h} \times \bar{r}) - r_p^2 \bar{v}}{e G_m^*} \quad (\text{B22a})$$

$$\bar{\nabla}_{\bar{r}} g = \frac{\frac{h}{G_m^*} (\bar{v} \times \hat{h}) - \hat{r} \frac{r_p^2}{r^2}}{e} \quad (\text{B22b})$$

It is easily shown that equation (B17) is satisfied for the gradients in equations (B22a) and (B22b). In fact, equation (B17) is satisfied for any function g of r , v , h , and $\bar{r} \cdot \bar{v}$. For such a function g ,

$$\bar{\nabla}_{\bar{v}}g = \frac{\partial g}{\partial v} \hat{v} + \frac{\partial g}{\partial h} (\hat{h} \times \bar{r}) + \frac{\partial g}{\partial(\bar{r} \cdot \bar{v})} \bar{r}$$

$$\bar{\nabla}_{\bar{r}}g = \frac{\partial g}{\partial r} \hat{r} + \frac{\partial g}{\partial h} (\bar{v} \times \hat{h}) + \frac{\partial g}{\partial(\bar{r} \cdot \bar{v})} \bar{v}$$

and

$$\begin{aligned} \bar{\nabla}_{\bar{v}}g \times \bar{v} + \bar{\nabla}_{\bar{r}}g \times \bar{r} &= \frac{\partial g}{\partial v} \bar{v} \times \bar{v} + \frac{\partial g}{\partial h} (\hat{h} \times \bar{r}) \times \bar{v} + \frac{\partial g}{\partial(\bar{r} \cdot \bar{v})} \bar{r} \times \bar{v} \\ &\quad + \frac{\partial g}{\partial r} \bar{r} \times \bar{r} + \frac{\partial g}{\partial h} (\bar{v} \times \hat{h}) \times \hat{r} + \frac{\partial g}{\partial(\bar{r} \cdot \bar{v})} \bar{v} \times \bar{r} = \bar{0} \end{aligned}$$

Hence the value of $\bar{\lambda} \times \bar{v} + \bar{\mu} \times \bar{r}$ is unaffected by the jump in $\bar{\lambda}$ and $\bar{\mu}$.

Conventional Case

As discussed in the RESULTS AND DISCUSSION section the circular parking orbit problem required additional analysis. For the conventional synchronous orbit case, it became obvious during the iteration that the trajectory was converging to a circular parking orbit. However, as the parking orbit became more and more nearly circular, it became increasingly more difficult to obtain convergence. The problem was traced to the gradients of perigee radius (eqs. (B22)). It is seen that the gradient becomes indeterminate as the eccentricity approaches zero. Attempts at resolving this indeterminacy showed that the indeterminacy is fundamental; that is, the gradient direction and magnitude are not defined for a circular orbit.

In order to resolve the indeterminacy and obtain convergence, the constraint was restated as requiring a circular orbit at the desired radius. This requires three constraints:

$$g_1 = r - r_d = 0 \tag{B23a}$$

$$g_2 = v - v_d = 0 \tag{B23b}$$

$$g_3 = \bar{r} \cdot \bar{v} = 0 \quad (\text{B23c})$$

The corresponding gradients are

$$\bar{\nabla}_{\bar{r}} g_1 = \hat{r}, \quad \bar{\nabla}_{\bar{v}} g_1 = \bar{0} \quad (\text{B24a})$$

$$\bar{\nabla}_{\bar{r}} g_2 = \bar{0}, \quad \bar{\nabla}_{\bar{v}} g_2 = \hat{v} \quad (\text{B24b})$$

$$\bar{\nabla}_{\bar{r}} g_3 = \bar{v}, \quad \bar{\nabla}_{\bar{v}} g_3 = \bar{r} \quad (\text{B24c})$$

Three jump scale factors are required for this case in order to converge on the intermediate conditions (eqs. (B24)). With this method, convergence was easily obtained.

It was verified that the optimum conventional case requires a circular parking orbit. This was accomplished by comparing the payload for a circular parking orbit case with the payloads for slightly noncircular parking orbits whose perigees are equal to the circular parking orbit altitude. A map of payload points was obtained which indicates that a circular parking orbit is optimum for this problem.

Boundary Value Problem

For the ATS-E mission, both fixed and optimum parking orbit coast times were considered. The transfer orbit coast time was always optimized, however, along with the durations of the first and second Centaur burns. Based on the preceding discussion of the transversality equation, the initial and final conditions for the two-point boundary value problem are shown in table I for the case where the parking orbit coast time was optimized.

If the desired final inclination is nonzero, then $(\bar{r} \cdot \hat{z})$ and $(\bar{v} \cdot \hat{z}) = 0$ in table I are replaced by i_d and $(\bar{\mu} \times \bar{r} + \bar{\lambda} \times \bar{v}) \cdot (\bar{r} \times \bar{v}) = 0$. If the parking orbit coast time is fixed, then an initial and final condition are removed. These are t_k and $\sum_{i=j}^{k-1} (S_i^f - S_{i+1}^o) = 0$. It should be recognized that there may be any number of fixed stages between t_j and t_k , etc. Also, the last three final conditions are evaluated at intermediate points in the trajectory.

For the ideal synchronous orbit mission, the two coast phases, as well as the three Centaur burns, were all optimized. The resulting initial and final conditions in the two-point boundary value problems are given in table II.

TABLE II. - INITIAL AND FINAL CONDITIONS

FOR CONVENTIONAL CASE

Initial conditions	Final conditions
ψ	E_d
$\dot{\psi}$	r_d
φ	\dot{r}_d
$\dot{\varphi}$	$r_{pk, d}$
ϵ_1	$v_{pk, d}$
ϵ_2	$(\bar{r} \cdot \bar{v})_{pk} = 0$
ϵ_3	$(\bar{r} \cdot \hat{z}) = 0$
t_j (first Centaur burn)	$(\bar{v} \cdot \hat{z}) = 0$
t_k (parking orbit coast)	$(\bar{\mu} \cdot \bar{v} + \bar{\lambda} \cdot \bar{G})_k = 0$
t_l (second Centaur burn)	$\sum_{i=j}^{l-1} (S_i^f - S_{i+1}^o) = 0$
t_m (transfer orbit coast)	$(\bar{\mu} \cdot \bar{v} + \bar{\lambda} \cdot \bar{G})_m = 0$
t_n (third Centaur burn)	$\sum_{i=j}^{n-1} (S_i^f - S_{i+1}^o) = 0$

TABLE I. - INITIAL AND FINAL CONDITIONS

FOR UNCONVENTIONAL CASE

Initial conditions	Final conditions
ψ	E_d
$\dot{\psi}$	r_d
φ	\dot{r}_d
$\dot{\varphi}$	$r_{p, d}$ (parking orbit)
ϵ	$(\bar{r} \cdot \hat{z}) = 0$
t_j (first Centaur burn)	$(\bar{v} \cdot \hat{z}) = 0$
t_k (parking orbit coast)	$\sum_{i=j}^{k-1} (S_i^f - S_{i+1}^o) = 0$
t_l (second Centaur burn)	$\sum_{i=j}^{l-1} (S_i^f - S_{i+1}^o) = 0$
t_m (transfer orbit coast)	$(\bar{\lambda} \cdot \bar{G} + \bar{\mu} \cdot \bar{v}) = 0$

As in the ATS-E case, if the final orbit inclination is nonzero then $(\bar{r} \cdot \hat{z}) = 0$ and $(\bar{v} \cdot \hat{z}) = 0$ in table II are replaced by i_d and $(\bar{\mu} \times \bar{r} + \bar{\lambda} \times \bar{v}) \cdot (\bar{r} \times \bar{v}) = 0$.

APPENDIX C

TWO-POINT BOUNDARY VALUE PROBLEM

The following technique was devised to systematically proceed from a simple, easily converged problem to the solution of the two-point boundary value problem for a circular synchronous equatorial orbit.

A trajectory is obtained to a slightly elliptical (parking) orbit with the desired perigee radius without plane change with a 90° launch azimuth. This problem converges easily. Then the ascent burn time is fixed at the value obtained and a variable length parking orbit coast, a fixed parking orbit perigee radius and second burn are added. This problem is targeted to the desired apogee and 180° argument of perigee for first equator crossing second burn. An inclination decrease of about 2° is then added to these final conditions and the problem is retargeted to the augmented final conditions. Now the transfer orbit coast (variable) and the apogee burn (fixed or variable) are added. This trajectory is integrated to the end with the converged initial guesses from the last step. The final conditions achieved will frequently be far from a circular synchronous equatorial orbit. However, specify the final conditions actually achieved as the desired ones, and optimize the problem. The parking orbit coast, second burn, and transfer orbit coast durations will change. Now alter the achieved final conditions toward the desired ones judiciously in steps, retargeting at each step. In this manner, the desired final orbit conditions may be obtained. Now the ascent burn duration may be optimized. If during the process of optimizing the ascent the parking orbit moves toward being circular, a fundamental difficulty is encountered in the equations for optimizing the problem with the perigee constraint. This is discussed further in appendix B and the RESULTS AND DISCUSSION section. Any sizable change in a constraint or final condition is best achieved by proceeding in steps. The problem is quite nonlinear. Attempts to obtain initial conditions as functions of the final conditions by extrapolation of data obtained from converged problems were made. They were generally unsuccessful.

REFERENCES

1. Hoelker, Rudolf F. ; and Silber, Robert: Injection Schemes for Obtaining a Twenty-Four Hour Orbit. *Aerospace Eng.*, vol. 20, no. 1, Jan. 1961, pp. 28-29, 76-84.
2. Rider, L. : Characteristic Velocity Requirements for Impulsive Thrust Transfer Between Non Co-Planar Circular Orbits. *ARS J.*, vol. 31, no. 3, Mar. 1961, pp. 345-351.
3. Teren, Fred; and Spurlock, Omer F. : Payload Optimization of Multistage Launch Vehicles. NASA TN D-3191, 1966.
4. Teren, Fred; and Spurlock, Omer F. : Optimal Three Dimensional Launch Vehicle Trajectories with Attitude and Attitude Rate Constraints. NASA TN D-5117, 1969.
5. Spurlock, Omer F. ; and Teren, Fred: A Trajectory Code for Maximizing the Payload of Multistage Launch Vehicles. NASA TN D-4729, 1968.
6. Clarke, Victor C. , Jr. : Constants and Related Data Used in Trajectory Calculations at the Jet Propulsion Laboratory. Tech. Rep. 32-273, Jet Propulsion Lab. , California Inst. Tech. , May 1, 1962.
7. Bliss, Gilbert A. : Lectures on the Calculus of Variations. Univ. Chicago Press, 1946.
8. Pontryagin, L. S. ; et al (K. N. Trirogoff, trans.): The Mathematical Theory of Optimal Processes. Interscience Publ. , 1962.
9. Dobson, Wilbur F. ; Huff, Vearl N. ; and Zimmerman, Arthur V. : Elements and Parameters of the Osculating Orbit and Their Derivatives. NASA TN D-1106, 1962.

FIRST CLASS MAIL



POSTAGE AND FEES PAID
NATIONAL AERONAUTICS
AND SPACE ADMINISTRATION

75 05U 001 55 51 3DS 70240 00903
AIR FORCE WEAPONS LABORATORY /WL0L/
KIRTLAND AFB, NEW MEXICO 87117

ATT E. LOU BOWMAN, CHIEF, TECH. LIBRARY

POSTMASTER: If Undeliverable (Section
Postal Manual) Do Not Return

"The aeronautical and space activities of the United States shall be conducted so as to contribute . . . to the expansion of human knowledge of phenomena in the atmosphere and space. The Administration shall provide for the widest practicable and appropriate dissemination of information concerning its activities and the results thereof."

— NATIONAL AERONAUTICS AND SPACE ACT OF 1958

NASA SCIENTIFIC AND TECHNICAL PUBLICATIONS

TECHNICAL REPORTS: Scientific and technical information considered important, complete, and a lasting contribution to existing knowledge.

TECHNICAL NOTES: Information less broad in scope but nevertheless of importance as a contribution to existing knowledge.

TECHNICAL MEMORANDUMS: Information receiving limited distribution because of preliminary data, security classification, or other reasons.

CONTRACTOR REPORTS: Scientific and technical information generated under a NASA contract or grant and considered an important contribution to existing knowledge.

TECHNICAL TRANSLATIONS: Information published in a foreign language considered to merit NASA distribution in English.

SPECIAL PUBLICATIONS: Information derived from or of value to NASA activities. Publications include conference proceedings, monographs, data compilations, handbooks, sourcebooks, and special bibliographies.

TECHNOLOGY UTILIZATION PUBLICATIONS: Information on technology used by NASA that may be of particular interest in commercial and other non-aerospace applications. Publications include Tech Briefs, Technology Utilization Reports and Notes, and Technology Surveys.

Details on the availability of these publications may be obtained from:

SCIENTIFIC AND TECHNICAL INFORMATION DIVISION
NATIONAL AERONAUTICS AND SPACE ADMINISTRATION
Washington, D.C. 20546